Journal of Coordination Chemistry

ISSN: 0095-8972 (Print) 1029-0389 (Online) Journal homepage: http://www.tandfonline.com/loi/gcoo20

Synthesis, solid-state structures, and urease inhibition activities of new copper(II) complexes based on O,N,O-tridentate Schiff bases

Yongming Cui, Lu Qiao, Yi Li, Hairui Jing, Yuguang Li & Qiang Wang

To cite this article: Yongming Cui, Lu Qiao, Yi Li, Hairui Jing, Yuguang Li & Qiang Wang (2016) Synthesis, solid-state structures, and urease inhibition activities of new copper(II) complexes based on O,N,O-tridentate Schiff bases, Journal of Coordination Chemistry, 69:15, 2318-2328, DOI: 10.1080/00958972.2016.1206199

To link to this article: http://dx.doi.org/10.1080/00958972.2016.1206199

JOURNAL OF COORDINATION CHEMISTRY, 2016
VOL. 69, NO. 15, 2318–2328
http://dx.doi.org/10.1080/00958972.2016.1206199

Taylor & Francis
Taylor & Francis Group

Synthesis, solid-state structures, and urease inhibition activities of new copper(II) complexes based on O,N,O-tridentate Schiff bases

Yongming Cui, Lu Qiao, Yi Li, Hairui Jing, Yuguang Li and Qiang Wang

Ministry of Education, Engineering Research Center for Clean Production of Textile Printing and Dyeing, Wuhan Textile University, Wuhan, PR China

ABSTRACT

Six new complexes of copper(II) coordinated with O,N,O-tridentate Schiff base dianions were synthesized and structurally characterized. The solid-state structures of **1**–**6** contain four-coordinate mononuclear copper(II) units with a slightly distorted square planar geometry. Complexes **1** and **4** derived from D-tyrosine have an infinite 1-D, right-handed helical chain, while **5** derived from L-tyrosine has an infinite 1-D, left-handed helical chain. Inhibitions of jack bean urease by **1**–**6** have been investigated, and potent inhibitory activities with IC_{50} range of 2.15 ± 0.11–32.12 ± 0.65 μM have been observed for these copper(II) complexes. A docking analysis using a DOCK program was conducted to position **4** into the jack bean urease active site to determine the probable binding conformation.

ARTICLE HISTORY
Received 1 January 2016
Accepted 13 May 2016

KEYWORDS
Copper(II) complexes; X-ray structures; urease inhibition; molecular docking

CONTACT Yuguang Li liyg2010@wtu.edu.cn; Qiang Wang qiang_wang@wtu.edu.cn
Supplemental data for this article can be accessed at http://dx.doi.org/10.1080/00958972.2016.1206199.

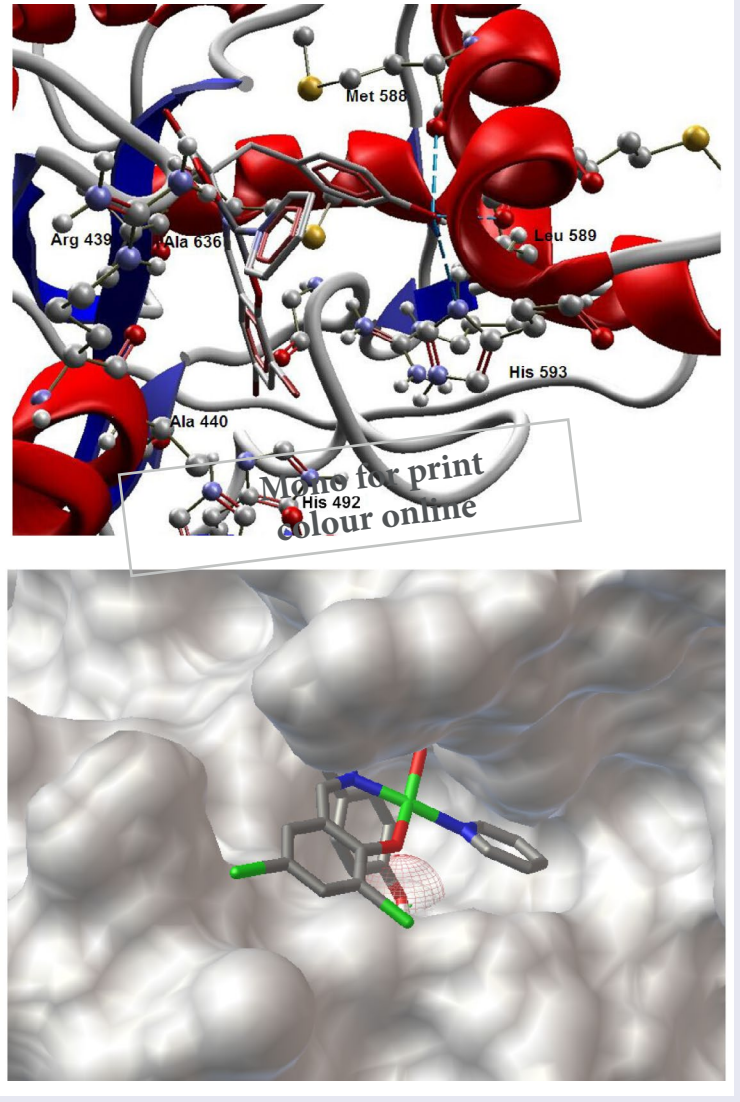

1. Introduction

The enzyme urease (urea amidohydrolase; E.C.3.5.1.5) contains two nickels at its active site and is known to hydrolyze urea to ammonia and carbon dioxide at a rate approximately 10^4 times the rate of the un-catalyzed reaction [1–4]. Hydrolysis of the reaction products results in an abrupt overall pH increase, responsible for negative effects of urease activity in human and animal health, as well as in agriculture. For example, urease has been shown to have virulence determinants in human and animal infections of the urinary and gastrointestinal tracts, being involved in the formation of infection stones, pyelonephritis, hepatic coma, and urinary catheter encrustation [5–7]. Urease in soils can lead to excessive volatilization of ammonia in urea fertilizer, since it degrades urea too rapidly [8, 9]. Urease inhibition studies have attracted attention in recent years; some urease inhibitors have been reported, such as phosphorodiamidates, hydroxamic acid derivatives, and imidazoles [10–12]. Unfortunately, some urease

inhibitors cannot be used *in vivo* because of their toxicity or instability [13]. Thus, it is interesting to synthesize new urease inhibitors with good activity and low toxicity.

Recently, a series of Schiff base metal complexes with potent inhibitory activities against urease have been synthesized by our group [14–16]. As a continuation of our work on Schiff base complexes as urease inhibitors, six mononuclear copper(II) complexes of Schiff base ligands derived from condensation of amino acids with different aldehyde compounds were synthesized. The inhibitory activities of the obtained complexes were tested against jack bean urease. The binding model of **4**, the strongest inhibition of urease in these Schiff base Cu complexes, with jack bean urease was simulated to validate its structure–activity relationship.

2. Experimental

2.1. Materials and physical measurements

Urease (from jack beans, type III, activity 22 units/mg solid), HEPES (Ultra) buffer and urea (molecular biology reagent) were from Sigma. 3,5-Dibromosalicylaldehyde and 5-chlorosalicylaldehyde were purchased from Aldrich and used without purification. Distilled water was used for all procedures. All experiments were performed at ambient temperature. Elemental analyses (C, N, and H) were performed using an Elementar Vario EL III elemental analyzer. Infrared spectra of solid samples were recorded using KBr pellets on a Nexus 870 FT-IR spectrophotometer between 4000 and 400 cm^{-1}. Electron spin resonance (ESR) spectra were recorded at room temperature using a Bruker ESR A-300 spectrometer with the following parameters: center field 3450 G, sweep width 1500 G, microwave frequency 9.86 G, modulation frequency 100 kHz, microwave power 1 mV. The enzyme inhibitory activity was measured on a Bio-Tek Synergy™ HT microplate reader.

2.2. Synthesis of the complexes

General procedure for the synthesis of O,N,O-tridentate Schiff bases and copper(II) complexes **1**–**6**: amino acid (2.0 mmol) was added to the solution of 3,5-dibromosalicylaldehyde (0.56 g, 2.0 mmol) [5-chlorosalicylaldehyde (345 mg, 2.0 mmol) or 2-hydroxy-1-naphthaldehyde (345 mg, 2.0 mmol)] in methanol (25 mL). The mixture was stirred for 30 min at ambient temperature to give an orange solution, which was added to a methanol solution (25 mL) of $Cu(NO_3)_2$ (0.340 g, 2 mmol) and two drops of pyridine/4-methyl-pyridine. The mixture was stirred for another 15 min at ambient temperature to give a clear solution and then filtered. The filtrate was kept in air for *ca*. 7 days to yield block crystals. The crystals were isolated, washed three times with distilled water, and dried in a vacuum desiccator containing anhydrous $CaCl_2$. H_2L^1, H_2L^2, H_2L^3, and H_2L^4 are shown in scheme 1.

2.2.1. [Cu(L^1)(pyridine)] (1)

Brown solid, X-ray quality single crystals were obtained, yield: 590.2 mg (62%). IR (KBr, cm^{-1}): 3447, 3246, 3055, 2961, 2930, 1617, 1602, 1588, 1538,1521, 1490, 1454, 1388, 1334, 1306, 1257, 1213, 1189, 1166, 1145, 1098, 1073, 1032, 972, 948, 901, 858, 832, 757, 676, 609, 450, 420. Anal. Calcd for $C_{25}H_{20}CuN_2O_4$: C, 63.03; H, 4.20; N, 5.89. Found: C, 63.08; H, 4.15; N, 5.72%.

2.2.2. [Cu(L^2)(pyridine)] (2)

Red-brown solid, yield: 678.8 mg (71%). IR (KBr, cm^{-1}): 3398, 3270, 3057, 2962, 2930, 2870, 1603, 1539, 1512, 1487, 1453, 1430, 1396, 1362, 1337, 1274, 1246, 1190, 1166, 1060, 1025, 968, 847, 824, 746, 641, 532, 512, 465, 426. Anal. Calcd for $C_{18}H_{19}CuN_3O_3$: C, 63.76; H, 4.60; N, 5.86. Found: C, 62.74; H, 4.44; N, 5.91%.

2.2.3. [Cu(L^2)(4-methyl-pyridine)] (3)

Red-brown solid, yield: 654.1 mg (69%). IR (KBr, cm^{-1}): 3521, 3194, 3060, 2935, 2851, 1676, 1626, 1541, 1511, 1457, 1435, 1417, 1399, 1363, 1345, 1305, 1284, 1182, 1092, 949, 937, 866, 825, 742, 650, 620,

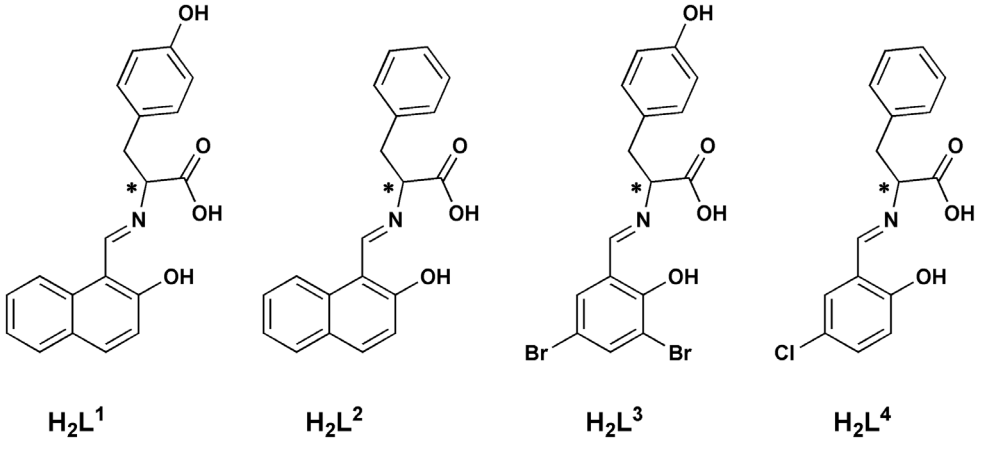

Scheme 1. Ligands H_2L^1, H_2L^2, H_2L^3 and H_2L^4.

567, 517, 487, 461, 415. Anal. Calcd for $C_{26}H_{22}CuN_2O_3$: C, 65.82; H, 4.64; N, 5.91. Found: C, 65.84; H, 4.60; N, 5.93%.

2.2.4. *[Cu(L³)(pyridine)]* (4)

Red-brown solid, yield: 852.2 mg (73%). IR (KBr, cm^{-1}): 3418, 3082, 2925, 2360, 1633, 1510, 1485, 1442, 1384, 1330, 1280, 1190, 1049, 939, 813, 769, 694, 619, 570. Anal. Calcd for $C_{21}H_{16}Br_2CuN_2O_4$: C, 43.21; H, 2.76; N, 4.80. Found: C, 43.10; H, 2.52; N, 4.93%.

2.2.5. *[Cu(L³)(4-methyl-pyridine)]* (5)

Red-brown solid, yield: 800.9 mg (67%). IR (KBr, cm^{-1}): 3247, 3054, 2962, 2929, 2872, 1618, 1603, 1519, 1491, 1453, 1389, 1366, 1334, 1306, 1256, 1214, 1187, 1163, 1147, 1072, 972, 829, 754, 698, 676, 660, 526, 477, 448. Anal. Calcd for $C_{22}H_{18}Br_2CuN_2O_4$: C, 44.17; H, 3.01; N, 4.68. Found: C, 44.20; H, 2.99; N, 4.64%.

2.2.6. *[Cu(L⁴)(4-methyl-pyridine)]* (6)

Red-brown solid, yield: 660.1 mg (72%). IR (KBr, cm^{-1}): 3521, 3186, 3060, 2935, 2851, 1676, 1626, 1541, 1511, 1457, 1435, 1417, 1399, 1363, 1345, 1305, 1284, 1182, 1082, 959, 937, 887, 815, 722, 646, 624, 577, 537, 477, 456, 420. Anal. Calcd for $C_{18}H_{19}Br_2CuN_3O_3$: C, 57.59; H, 4.15; N, 6.11. Found: C, 57.55; H, 4.18; N, 6.13%.

2.3. Crystal structure determinations

X-ray crystallographic data were collected on a Bruker SMART Apex II CCD diffractometer using graphite-monochromated Mo-Kα (λ = 0.71073 Å) radiation [17, 18]. The collected data were reduced using SAINT, and empirical absorption corrections were performed using SADABS. The structures were solved by direct methods and refined against F^2 by full-matrix least squares using SHELXTL version 6.1. All non-hydrogen atoms were refined anisotropically. All hydrogens were placed in geometrically ideal positions and constrained to ride on their parent atoms.

2.4. Measurement of jack bean urease inhibitory activity

The measurement of urease activity was carried out according to the procedure reported by Tanaka [19]. Generally, the assay mixture containing 25 µL of jack bean urease (12 kU L^{-1}) and 25 µL of the test complexes with the concentration range of 0.5–7.5 µM (dissolved in DMSO : H_2O = 1 : 1 v/v) was

preincubated for 1 h at 37 °C in a 96-well assay plate. After preincubation, 200 µL of 100 mM HEPES (4-(2-hydroxyerhyl)piperazine-1-erhanesulfonic acid) buffer pH 6.8 containing 500 mM urea [20] and 0.002% phenol red was added and incubated at 37 °C. The reaction was measured with a microplate reader (560 nm), where an increase in the pH value from 6.8 to 7.7 for the HEPES buffer was determined by the color change of the phenol red indicator [21].

2.5. Docking simulations

Molecular docking of the inhibitor with the 3-D structure of jack bean urease (entry 3LA4 in the Protein Data Bank) was carried out using the DOCK 4.2 program suite [22–24]. The graphical user interface AutoDockTools (ADT 1.4.5) was performed to setup inhibitor–enzyme interactions, where all hydrogens were added. Gasteiger charges were calculated, and nonpolar hydrogens were merged to carbons. The Ni initial parameters were set as $r = 1.170$ Å, $q = +2.0$, and van der Waals well depth of 0.100 kcal mol^{-1} [25]. As performed by the graphical user interface AutoDockTools, the catalytic center and the peripheral anionic site of the target protein were scanned to evaluate the binding mode of the inhibitor–urease complex. The flexible docking of the ligand structures was done by the Lamarckian genetic algorithm, searching for favorable bonding conformations of the ligands at the sites of the target protein. The docking procedure of complex with the enzyme active site of jack bean urease was performed as described previously [26].

3. Results and discussion

3.1. Synthesis

All the complexes were prepared from reactions of 3,5dibromosalicylaldehyde/5-chlorosalicylaldehyde or 2-hydroxy-1-naphthaldehyde with L-tyrosine/phenylalanine, pyridine/4-methyl-pyridine and copper(II) chloride. The obtained complexes were microcrystalline solids which were stable in air with melting points above 200 °C. They were soluble in organic solvents such as methanol, DMF, and DMSO. Copper ions in **1**–**6** were coordinated by oxygen and nitrogen donors from two Schiff base ligands. The elemental analyses were in agreement with the chemical formula proposed for **1**–**6**.

3.2. IR analysis and ESR spectra

The Schiff base complexes **1**–**6** were characterized by single-crystal X-ray diffraction, FT-IR spectroscopy, and elemental analysis. IR spectra of these complexes exhibit strong absorptions at 1633–1603 cm^{-1}, assignable to ν(C=N) [27]. The C=N groups in **1**–**6** show strong absorptions at 1617, 1603, 1626, 1633, 1618, and 1626 cm^{-1}, respectively. Due to the impact of metal atoms, the amino-absorption peaks of the Schiff base ligands shift to lower wavenumber. In addition, the broad strong absorption between 1521 and 1512 could be attributed to the C=C backbone stretching vibration in the benzene ring. Several weak bands at 3000–2800 cm^{-1} were most likely due to aromatic C–H groups. These Schiff base complexes were confirmed by additional weak bands at 487–415 and 577–512 cm^{-1}, which were attributed to $\nu_{(M-O)}$ [28]. The EPR spectrum of **5** clearly indicates a slightly distorted square planar geometry of the copper(II) center ($g_{\parallel} = 2.144$, $g_{\perp} = 2.043$, see figure S7), which is compared with that of a copper(II) center ($g_{\parallel} = 2.226$, $g_{\perp} = 2.064$) in the literature [29].

3.3. Crystal structure description

The molecular structures of **1**–**6** determined by single-crystal X-ray diffraction are shown in figures 1–3. These copper(II) complexes adopt square planar coordination geometries and comprise mononuclear four-coordinate copper(II) units with a general formula of CuLX, in which X is a monodentate ligand (X = pyridine for **1**, **2**, and **4**, and 4-methylpyridine for **3**, **5**, and **6**). L is the O,N,O-tridentate Schiff base

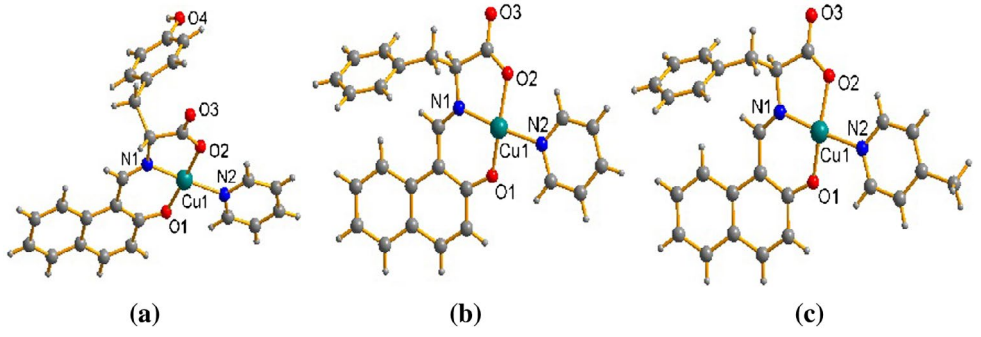

Figure 1. (a) *Ball-and-stick* representation of molecular structure for **1**; (b) *Ball-and-stick* representation of molecular structure for **2**; (c) *Ball-and-stick* representation of molecular structure for **3**.

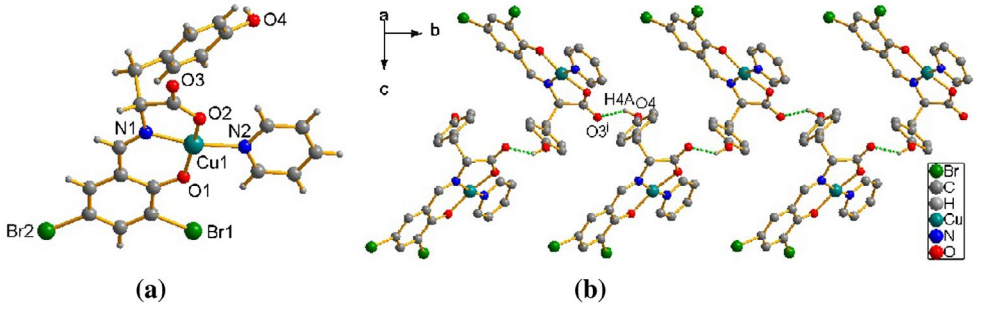

Figure 2. (a) *Ball-and-stick* representation of molecular structure for **4**; (b) The 1-D right-handed helical chain of **4** (symmetric code: (i) $1/2 - x, -1/2 + y, 7/4 - z$).

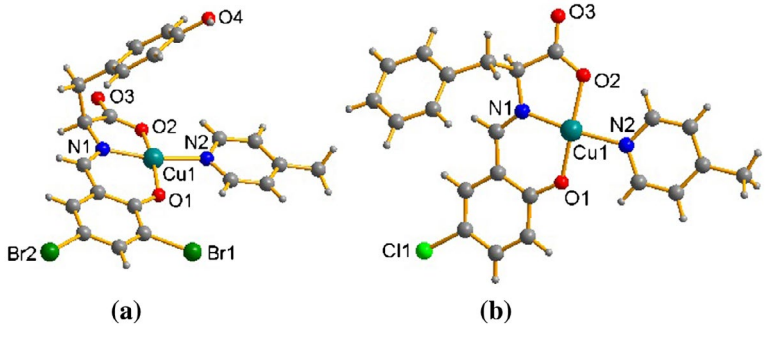

Figure 3. (a) *Ball-and-stick* representation of molecular structure for **5**; (b) *Ball-and-stick* representation of molecular structure for **6**.

dianion which was derived from D-tyrosine (L^1 in **1**, L^3 in **4**), L-tyrosine (L^3 in **5**), and L-phenylalanine (L^2 in **2** and **3**, L^4 in **6**), respectively. Crystallographic data of **1**–**6** are given in table 1. Selected bond distances and angles are given in table 2.

Single-crystal X-ray diffraction analysis reveals that **1** crystallizes in the monoclinic space group $P2_1/c$ (No. 14). H_2L^1 derived from condensation of 2-hydroxy-1-naphthaldehyde and D-tyrosine, in the presence of pyridine, forms the four-coordinate Cu(L^1)(pyridine), where L^1 is the tridentate Schiff base dianion (figure 1(a)). In the Cu(L^1)(pyridine), the coordination environment of the copper(II) is square planar, with O,N,O-donors of the L^1 dianion and a N of pyridine. Complex **1** has a τ_4 value of 0.05 in a CuN_2O_2 chromophore, supporting the assignment of square planar geometry [30, 31]. The Cu(L^1)

Table 1. Crystal data for **1**–**6**.

Complex	1	2	3	4	5	6
Empirical formula	$C_{25}H_{20}CuN_2O_4$	$C_{25}H_{22}CuN_2O_4$	$C_{26}H_{22}CuN_2O_3$	$C_{21}H_{16}Br_2CuN_2O_4$	$C_{22}H_{18}Br_2CuN_2O_4$	$C_{22}H_{19}ClCuN_2O_3$
Molecular weight	475.97	477.99	474.00	583.72	597.74	458.38
Crystal system	Monoclinic	Monoclinic	Monoclinic	Tetragonal	Monoclinic	Orthorhombic
Space group	$P2_1/c$	$P2_1$	$P2_1$	$P4_32_12$	$P2_1$	$P2_12_12$
a (Å)	8.5871(7)	10.2706(4)	10.0945(10)	10.7451(11)	9.6228(10)	14.789(2)
b (Å)	12.8439(10)	5.2969(3)	5.2955(6)	10.7451(11)	12.4415(13)	9.3378(14)
c (Å)	19.2723(13)	20.1325(9)	20.322(2)	36.473(4)	18.1188(19)	14.398(2)
α (°)	90.00	90.00	90.00	90.00	90.00	90.00
β (°)	107.071(3)	102.307(2)	100.883(2)	90.00	95.647(2)	90.00
γ (°)	90.00	90.00	90.00	90.00	90.00	90.00
T (K)	291(2)	291(2)	291(2)	291(2)	291(2)	291(2)
V (Å^3)	2031.9(3)	1070.09(9)	1066.79(19)	4211.0(7)	2158.7(4)	1988.3(5)
Z	4	2	2	8	4	4
ρ_{Calcd} (g cm^{-3})	1.556	1.483	1.476	1.841	1.839	1.531
F (0 0 0)	980	494	490	2296	1180	940
μ (Mo-K$_\alpha$) (mm^{-1})	1.112	1.737	1.055	4.864	4.746	1.259
Data/restraint/parameters	3985/0/289	2563/1/289	3917/1/290	3568/0/275	7282/1/563	3898/0/263
Goodness of fit on F^2	1.006	1.010	1.017	1.012	1.015	1.012
Final R_1, wR_2 [$I > 2\sigma(I)$]	0.0566, 0.1047	0.0284, 0.0725	0.0213, 0.0567	0.0463, 0.1114	0.0278, 0.0620	0.0193, 0.0522

Table 2. Selected bond lengths (Å) and angles (°) for **1**–**6**.

1			
Cu1–O1	1.874(2)	Cu1–N1	1.926(3)
Cu1–O2	1.924(3)	Cu1–N2	2.024(3)
O1–Cu1–O2	176.41(12)	N1–Cu1–N2	175.90(13)
2			
Cu1–O1	1.900(2)	Cu1–N1	1.932(2)
Cu1–O2	1.954(2)	Cu1–N2	2.014(3)
O1–Cu1–O2	163.72(10)	N1–Cu1–N2	174.64(12)
3			
Cu1–O1	1.9110(14)	Cu1–N1	1.9359(14)
Cu1–O2	1.9528(14)	Cu1–N2	2.0155(15)
O1–Cu1–O2	162.29(6)	N1–Cu1–N2	175.51(7)
4			
Cu1–O1	1.879(5)	Cu1–N1	1.907(6)
Cu1–O2	1.936(5)	Cu1–N2	1.997(6)
O1–Cu1–O2	166.8(2)	N1–Cu1–N2	169.1(3)
5			
Cu1–O1	1.903(3)	Cu1–N1	1.924(4)
Cu1–O2	1.938(3)	Cu1–N2	1.994(4)
Cu2–O5	1.896(3)	Cu2–N3	1.936(4)
Cu2–O6	1.952(3)	Cu2–N4	1.984(4)
O1–Cu1–O2	167.56(13)	N1–Cu1–N2	169.73(15)
O5–Cu2–O6	165.66(14)	N3–Cu2–N4	167.17(15)
6			
Cu1–O1	1.9043(12)	Cu1–N1	1.9403(14)
Cu1–O2	1.9506(11)	Cu1–N2	2.0319(15)
O1–Cu1–O2	169.59(5)	N1–Cu1–N2	171.55(5)

(pyridine) molecules are interconnected through intermolecular O–H···O hydrogen bonds between the phenol OH of the tyrosine and two carboxylic oxygens (O2 and O3) of the adjacent molecule, {O4–H4···O2$^{\#}$ = 3.033(4) Å, 118.7° and O4–H4···O3$^{\#}$ = 2.803(4) Å, 159.2°}. This leads to an infinite 1-D, right-handed helical chain.

In contrast to **1**, both **2** and **3** crystallize in the monoclinic space group $P2_1$ (No. 4). Complex **2** with pyridine crystallizes with water of crystallization when compared with **3** with 4-methylpyridine. The molecular structures of **2** and **3** consist of mononuclear four-coordinate copper(II) units, [Cu(L^2)(pyridine)]·H_2O and Cu(L^2)(4-methylpyridine), respectively, as depicted in figures 1(b) and (c). The coordination geometry around copper in **2** is strikingly similar to that in **3**, both showing slightly distorted square planar geometry with the L^2 dianion a O,N,O-tridentate ligand derived from L-phenylalanine. Complexes **2** and **3** have the corresponding τ_4 values of 0.15 and 0.16 in a CuN_2O_2 chromophore, supporting the assignment of a distorted square planar geometry. The four-coordinate copper centers in **2** and **3** are further linked through the carboxyl O from an adjacent molecule occupying the apical site, Cu1–O3# = 2.466(3) Å in **2** and 2.501(3) Å in **3**. The coordination sphere around copper(II) in **2** and **3** can be described as a slightly distorted square pyramidal with the respective τ_5 values of 0.18 and 0.22 [32]. This contact leads to an infinite 1-D zigzag chain in the solid-state structures of **2** and **3**. In addition, the lattice water molecules in **2** are connected by hydrogen bonding interactions {O4–H4B···O4# = 2.900(4) Å, 111.3°}, which leads to an infinite 1-D water chain. Such an infinite water chain is further linked with two neighboring zigzag chains by hydrogen bonds between the carboxylate O3 of the tridentate L^2 dianion and lattice water molecules, {O4–H4A···O3# = 2.818(3) Å, 140.1°}, to generate an infinite 1-D ladder-like structure of **2**.

Complexes **4** and **5** crystallize in the tetragonal space group $P4_32_12$ (No. 96) and the monoclinic space group $P2_1$ (No. 4), respectively. The crystal structures of **4** and **5** are shown in figures 2(a) and 3(a). In the asymmetry unit, **4** presents a [Cu(L^3)(pyridine)] molecule, while **5** contains two independent [Cu(L^3)(4-methylpyridine)] molecules. X-ray crystallographic studies have shown that both **4** and **5** contain copper in a slightly distorted square planar geometry with a CuN_2O_2 chromophore. The coordination sites are occupied by O,N,O-donors from L^3 dianion and a pyridine (**4**) or 4-methylpyridine (**5**). The τ_4 values for the CuN_2O_2 chromophore are 0.17 in **4** and 0.16 and 0.19 in **5**, respectively. This supports an assignment of the distorted square planar geometry of **4** and **5**. Similar to **1**, the Cu(L^3) (pyridine) molecules of **4** derived from D-tyrosine are linked into an infinite 1-D, right-handed helical chain by intermolecular O–H···O hydrogen bonds between the phenol OH groups of D-tyrosines and one carboxylic O3 of adjacent molecules, {O4–H4A···O3# = 2.690(9) Å, 140.2°} (figure 2(b)). [Cu(L^3)(4-methylpyridine)] molecules of **5** derived from L-tyrosine are linked into an infinite 1-D, left-handed helical chain by intermolecular O–H···O hydrogen bonds between the phenol OH groups of the L-tyrosines and the carboxylate oxygens (O3 and O8) of adjacent molecules, {O4–H4A···O3# = 2.698(5) Å, 164.7° for Cu1 and O8–H8A···O7# = 2.744(4) Å, 165.1° for Cu2}.

The space group of **6** was determined to be $P2_12_12$ (No. 18). The crystal structure of **6**, shown in figure 3(b), is structurally very similar to **3**. The tridentate Schiff base ligand (H_2L^4) derived from condensation of 5-chlorosalicylaldehyde and L-phenylalanine, in the presence of 4-methylpyridine, forms the four-coordinate Cu(L^4)(4-methylpyridine), where L^1 is a tridentate dianion. This leads to a square planar CuN_2O_2 chromophore with τ_4 value of 0.13. In the solid state, an infinite zigzag chain of **6** is also achieved, owing to the apical position occupied by a carboxylate O3 from an adjacent molecule, Cu1–O3# = 2.449(3) Å.

3.4. Inhibitory activity against jack bean urease

The urease inhibiting abilities of **1**–**6** were studied by testing their IC_{50} values against jack bean urease (see table 3). Compared with the standard inhibitor acetohydroxamic acid (AHA, IC_{50} = 63.70 μM), the copper(II) complexes **1**–**6** display potent inhibitory activities (IC_{50} = 2.15–32.12 μM) against jack bean urease. The strong urease inhibiting ability exhibited by the copper(II) complexes is due to the strong Lewis acid properties of copper ion [33].

Inhibitory strength of the six copper(II) complexes toward jack bean urease decreases in the order **4** > **5** > **6** > **2** > **3** > **1**. Among the six copper(II) complexes tested, **4**, **5**, and **6** derived from salicylaldehyde with halogen substitution are much more potent than those of **1**, **2**, and **3** derived from 2-hydroxy-1-naphthaldehyde. This defines the pattern of halogen (Br or Cl) substitution in the aromatic ring for obtaining potent activities.

Complexes **4** and **5** exhibit stronger ability to inhibit urease than **6** although they all have halogen substitution. This indicates that Br-substitution in the aromatic ring is advantageous for obtaining potent activity compared to Cl-substitution. This result is consistent with our previous study [34]. Although the crystal structures of **2**, **3**, **4**, and **5** are very similar except for the 4-methyl substitution on pyridine, the urease inhibiting abilities of **4** and **2** are higher than those of **5** and **3**, respectively. The results suggest that methyl substitution will make the molecular chain longer and decrease the activity.

3.5. Molecular docking study

X-ray structure of the native jack bean urease (entry 3LA4 in the Protein Data Bank) shows that the two nickels are surrounded by His407, His409, Lys490, His492, Asp494, His519, His545, Cys592, His593, Arg 609, Asp633, and Ala636 [35]. Molecular docking of **4** into the active site of jack bean urease was performed on the binding model based on the jack bean urease structure (3LA4.pdb). This provides understanding of the present inhibitory activity of the complex against jack bean urease.

The binding model of **4** at the active site of jack bean urease is depicted in figure 4. All the amino acid residues which had interactions with urease are shown in figure 4. In the **4**-urease

Table 3. Inhibition of jack bean urease by **1**–**6** and AHA.

Tested materials	IC_{50} (μM)
1	32.12 ± 0.65
2	22.50 ± 1.01
3	27.32 ± 0.31
4	2.15 ± 0.11
5	4.25 ± 0.54
6	8.80 ± 1.02
Acetohydroxamic acid	60.22 ± 0.85

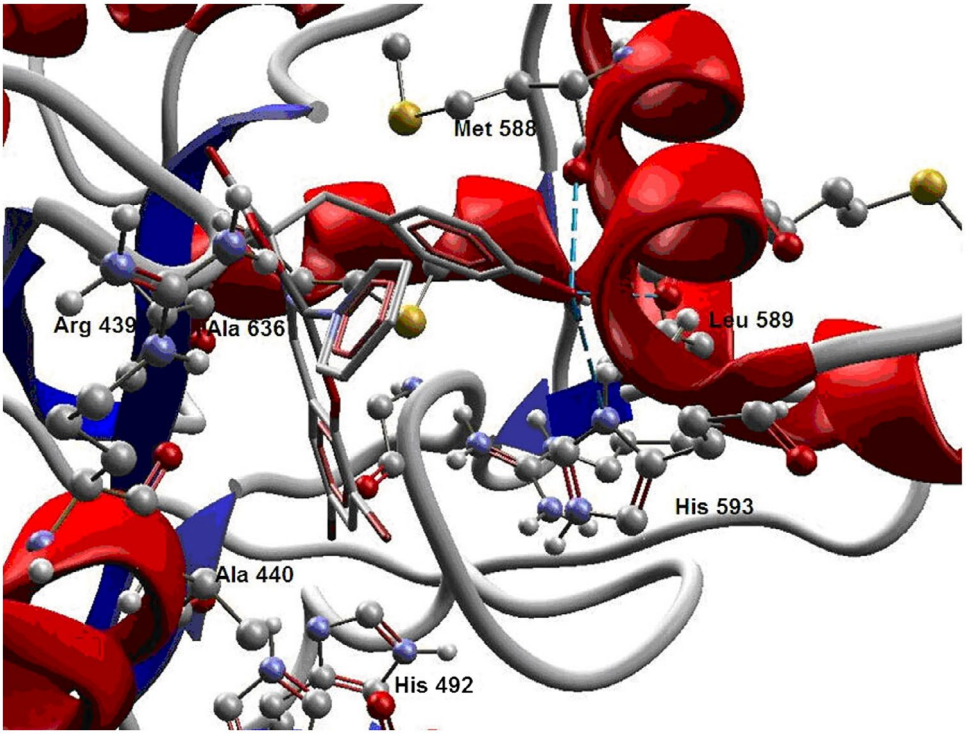

Figure 4. The binding model of **4** at the active site of jack bean urease.

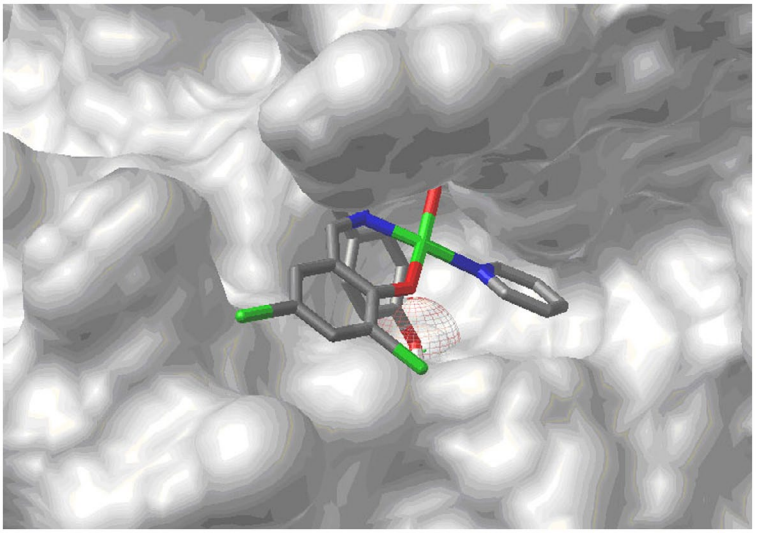

Figure 5. The docking model of enzyme surface structure of **4**-urease complex.

model, three hydrogen bonds were formed. One formed between the oxygen of **4** and the amino hydrogen of His593 (length of the hydrogen bond: His593N–H···O_4 = 3.111(7) Å, energy of the hydrogen bond: His593 N–H···O_4 = −2.1864). The other two hydrogen bonds formed between the hydroxyl group of **4** and oxygens of Met588 with Leu589, respectively (length of the hydrogen bonds: Met588O···OH_4 = 2.944(3) Å, Leu589O···OH_4 = 2.5042 Å; energy of the hydrogen bonds: Met588O···OH_4 = −2.5, Leu589O···OH_4 = −1.7016). Moreover, **4** might form hydrophobic interactions with Leu 589, Ala 440, and Ala 636, respectively. The urease inhibitory property may be attributed to the above hydrogen bonds and hydrophobic interactions formed between these ligands and urease.

The docking model of the enzyme surface structure of **4**-urease complex is shown in figure 5. Complex **4** filled in the active pocket of the urease. The results of molecular docking study could explain the inhibitory activity of the complex against jack bean urease.

4. Conclusion

This paper describes the synthesis, crystal structures, and urease inhibitory activities of six new copper(II) complexes with O,N,O-tridentate Schiff base ligands. These copper(II) complexes exhibited good inhibitory activity against jack bean urease. The docking calculations revealed that the Schiff base-copper(II) complexes have potential as urease inhibitors. The results in this work are in accord with studies reported earlier, where some Cu(II) complexes have stronger urease inhibitory activities to urease, with IC_{50} ranging from 0.1 to 50 μM [15, 33, 36–39]. Compared with the data reported before, the complexes reported in this study exhibit strong inhibitory activity to urease and may be used as urease inhibitors. Detailed investigations are continuing to study the mechanisms of the inhibitory activity.

Supplementary material

CCDC numbers 887876 (**1**), 887877 (**2**), 887878 (**3**), 1416455 (**4**), 887880 (**5**), and 887879 (**6**) contain the supplementary crystallographic data (CIF) for this article. These data can be obtained free of charge via http://www.ccdc.cam.ac.uk/conts/retrieving.html or from the Director, CCDC, 12 Union Road, Cambridge CB2 1EZ, UK (Fax: +44-1223-336-033; E-mail: deposit@ccdc.cam.ac.uk).

Disclosure statement

No potential conflict of interest was reported by the authors.

Funding

This work was supported by the National Natural Science Foundation of China [grant number 21101122], [grant number 21277106]; the Collaborative Innovation Plan of Hubei Province for Key Technology of Eco-Ramie Industry; State Scholarship Fund of China [grant number 201408420061].

References

[1] L.S.B. Upadhyay. *Indian J. Biotechnol.*, **11**, 381 (2012).
[2] R.P. Hausinger. *Biochemistry of Nickel*, Plenum Press, New York (1993).
[3] D. Witkowska, M. Rowinska-Zyrek, G. Valensin, H. Kozlowski. *Coord. Chem. Rev.*, **256**, 133 (2012).
[4] E. Jabri, M.B. Carr, R.P. Hausinger, P.A. Karplus. *Science*, **268**, 998 (1995).
[5] H.L.T. Mobley, R.P. Hausinger. *Microbiol. Rev.*, **53**, 85 (1989).
[6] H.L.T. Mobley, M.D. Island, R.P. Hausinger. *Microbiol. Rev.*, **59**, 451 (1995).
[7] M.J. Todd, R.P. Hausinger. *Biochemistry*, **39**, 5389 (2000).
[8] V.L. Lockamy, J. Huang, H. Shields, S.K. Ballas, S.B. King, D.B. Kim-Shapiro. *Biochim. Biophys. Acta*, **1622**, 109 (2003).
[9] G. Estiu, K.M. Merz. *Biochemistry*, **45**, 4429 (2006).
[10] S. Ciurli, S. Benini, W.R. Rypniewski, K.S. Wilson, S. Miletti, S. Mangani. *Coord. Chem. Rev.*, **331**, 190 (1999).
[11] M. Biglar, K. Soltani, F. Nabati, R. Bazl, F. Mojab, M. Amanlou. *Iran. J. Pharm. Res.*, **11**, 831 (2012).
[12] S. Vassiliou, P. Kosikowska, A. Grabowiecka, A. Yiotakis, P. Kafarski, L. Berlicki. *J. Med. Chem.*, **53**, 5597 (2010).
[13] M. Font, M.J. Domínguez, C. Sanmartín, J.A. Palop, S. San-Francisco, O. Urrutia, F. Houdusse, J.Mkk. García-Mina. *J. Agric. Food Chem.*, **56**, 8451 (2008).
[14] Y. Li, Z. Li, Y. Liu, X. Dong, Y.Cui. *J. Coord. Chem.*, **65**, 19 (2012).
[15] X. Dong, Y. Li, Z. Li, Y. Cui, H. Zhu. *J. Inorg. Biochem.*, **108**, 22 (2012).
[16] W. Chen, Y. Li, Y. Cui, X. Zhang, H. Zhu, Q. Zeng. *Eur. J. Med. Chem.*, **45**, 4473 (2010).
[17] G.M. Sheldrick, *SMART (version 5.0), SAINT (version 6.0), SHELXTL (version 6.1), SADABS (version 2.03)*. Bruker AXS, Madison, Wisconsin, USA (2000).
[18] G.M. Sheldrick. *Acta Crystallogr.*, **A64**, 112 (2008).
[19] T. Tanaka, M. Kawase, S. Tani. *Life Sci.*, **73**, 2985 (2003).
[20] W. Zaborska, B. Krajewska, Z. Olech. *J. Enzyme Inhib. Med. Chem.*, **19**, 65 (2004).
[21] Y.M. Cui, W.T. Liu, Y. Liu, W. Chen, Y.G. Li. *J. Coord. Chem.*, **64**, 3960 (2011).
[22] R. Huey, G.M. Morris, A.J. Olson, D.S. Goodsell. *J. Comput. Chem.*, **28**, 1145 (2007).
[23] A. Balasubramanian, K. Ponnuraj. *J. Mol. Biol.*, **400**, 274 (2010).
[24] G. Estiu, D. Suárez, K.M. Merz. *J. Comput. Chem.*, **27**, 1240 (2006).
[25] F. Musiani, E. Arnofi, R. Casadio, S. Ciurli. *J. Biol. Inorg. Chem.*, **6**, 300 (2001).
[26] Y. Cui, X. Dong, W. Chen, W. Wang, Y. Li, H. Zhu. *J. Enzyme Inhib. Med. Chem.*, **27**, 528 (2012).
[27] K. Cheng, Z. You, H. Zhu. *Aust. J. Chem.*, **60**, 375 (2007).
[28] A. Torreggiani, M. Tamba, G. Fini. *Biopolymers*, **57**, 149 (2000).
[29] T. Tano, M.Z. Ertem, S. Yamaguchi, A. Kunishita, H. Sugimoto, N. Fujieda, T. Ogura, C.J. Cramer, S. Itoh. *Dalton Trans.*, **40**, 10326 (2011).
[30] L. Yang, D.R. Powell, R.P. Houser. *Dalton Trans.*, **9**, 955 (2007).
[31] P.R. Raithby, G.P. Shields, F.H. Allen, W.D.S. Motherwell. *Acta Cryst.*, **B56**, 444 (2000).
[32] A.W. Addison, T.N. Rao, J. Reedijk, J. van Rijn, G.C. Verschoor. *J. Chem. Soc. Dalton Trans.*, 1349 (1984).
[33] D.A. Evans, S.J. Miller, T. Lectka, P. von Matt. *J. Am. Chem. Soc.*, **212**, 7559 (1999).
[34] Y. Cui, X. Dong, Y. Li, Z. Li, W. Chen. *Eur. J. Med. Chem.*, **58**, 323 (2012).
[35] N.C. Ha, S.T. Oh, J.Y. Sung, K.A. Cha, M.H. Lee, B.H. Oh. *Nat. Struct. Biol.*, **8**, 505 (2001).
[36] H. Zhu, Z.Z. Wang, B. Qi, T. Huang, H.L. Zhu. *J. Coord. Chem.*, **66**, 2980 (2013).
[37] Z.M. Yang, H. Zhu, J. Sun, S.S. Qian, M.N. Cai, H.L. Zhu. *J. Coord. Chem.*, **66**, 2736 (2013).
[38] G.H. Sheng, Q.C. Zhou, X.M. Hu, C.F. Wang, X.F. Chen, D. Xue, K. Yan, S.S. Ding, J. Wang, Z.Y. Du, Z.H. Liu, C.Y. Zhang, H.L. Zhu. *J. Coord. Chem.*, **68**, 1571 (2015).
[39] G.H. Sheng, Q.C. Zhou, J. Sun, X.S. Cheng, S.S. Qian, C.Y. Zhang, Z.L. You, H.L. Zhu. *J. Coord. Chem.*, **67**, 1265 (2014).